Automating a Wheel Manufacturing Operation

To overcome dimensional inaccuracies on joints in large agricultural wheels, an automated gas metal arc welding cell was developed

BY J. C. DUTRA, N. G. BONACORSO, D. ERDMANN DOS SANTOS, M. H. HEMMER, AND R. H. GONÇALVES E SILVA

Rice is among the most important cereals in the world. Developing countries account for 95.2% of world consumption and 95.9% of production. According to data released in 2006 by the Food and Agriculture Organization of the United Nations, Asia is the largest producer (90.5%), followed by the Americas (5.9%), Africa (3.0%), Europe (0.5%), and Oceania (0.1%).

Irrigated farming, an ecosystem of wetlands, is the predominant method for growing rice around the world. In this type of cultivation, the earth is kept submerged for the greater part of the time the rice is growing, with the water removed only a few days before harvest. To work on this type of terrain, several companies have adapted tractors with high, thin-steel wheels to facilitate movement of the tractor in the flooded rice fields and minimize damage to the crop — Fig. 1.

In recent decades, companies manufacturing agricultural implements have sought improvements in their production processes in order to compete in terms of technology and also to compete in foreign markets. These manufacturing companies undertake development of new projects either using their own staff or by partnering

J. C. DUTRA (jdutra@labsolda.ufsc.br), *D. ERDMANN DOS SANTOS* (d.santos@labsolda.ufsc.br), *and R. H. GONÇALVES E SILVA* (regis@labsolda.ufsc.br) *are with Federal University of Santa Catarina, Mechanical Engineering Department, Florianópolis, SC, Brazil. N. G. BONACORSO* (nelso@ifsc.edu.br) *is with Federal Institute of Education, Science and Technology of Santa Catarina, Department of Metal Mechanics, Florianópolis, SC, Brazil. M. H. HEMMER* (helio@braselio.com.br) *is with Company Brasélio, Department of Industrial Design, Massaranduba, SC, Brazil.*

Fig. 1 — Farm tractor with metallic wheels.

with research centers. Thus, welding procedures and equipment have gained prominence and are objects of technological innovations and adaptations.

The application of welding to produce the tractors metal wheels is an example of seeking a solution to increase quality and productivity. In Brazil, the metal wheels are produced using thin sheets and thick flat bars. The manufacturing processes involved include cutting, forming, assembling, welding, and finishing (Ref. 1). The mounting step, as shown in Fig. 2, is performed manually by tack welding structural components on both sides of the wheels using gas metal arc welding (GMAW).

For one manufacturer, assembling a wheel requires 16 joints to be welded together, eight each side, as shown in Fig. 3. Each side has six radial joints (labeled JR1, JR2, ..., JR6), an inner circumference joint (JCI), and an outer circumference joint (JCE).

The radial joints (labeled JR in Fig. 3) are formed by joining two thin plates that are initially bent at 90 deg and fixed side by side forming a V-shaped opening. Both joints, JCI and JCE, are angles formed by the intersection of thin plates with a thick, flat bar.

Due to the characteristics of the soil and the type of tractor used, various kinds of wheels with differing dimensions are manufactured. Considering the three types of joints in the existing wheels (JR, JCI, and JCE), the smallest wheel has a total weld length 10.84 m per side while the largest wheel has a total weld length of 12.64 m per side.

In these types of joints, the average manual welding speed is approximately 550 mm/min resulting in a welding time range per side of 20 to 23 min. However, the productivity per day, for each eight-h shift and each welder, is only six wheels, because approximately 40 min are required to weld each side of the wheel. Moreover, there is a need for additional welding work in approximately half the wheels to ensure tightness and to avoid premature oxidation due to water infiltration.

Incomplete fusion and small undercuts in the welded joints are the welding defects that give the greatest financial losses to farmers and companies manufacturing the wheels. Those defects cannot be detected during manufacture, nor by visual inspection and a seal test, but only when mechanical stresses arising from use result in sealing failures. In turn, loss of tight-

Fig. 2 — The GMAW process is used to tack weld this steel wheel assembly.

ness is what decreases wheel life because of internal oxidation.

The root cause of these defects, especially in circumferential joints (Fig. 4), is the complexity of the welder having to manually manipulate the GMAW gun. To avoid undercuts or puncturing the thin plate, the welder guides the arc toward the thick, flat bar, producing a weld that melts the thin sheet less. On the other hand, to ensure good fusion of the thin plate, the welder guides the arc to them, thereby generating small undercuts.

Furthermore, the difficulty of manipulating the gun is increased due to the existence of variations in joint root openings — Fig. 4. In this case, the welder uses an oscillating motion to reduce direct action of the arc on the joint to stretch the molten pool, and thus prevent the arc from puncturing the thin plate (Ref. 2).

Given these problems, development of an automatic, flexible welding cell for producing defect-free joints and to increase productivity is the challenge and motivating factor for the execution team.

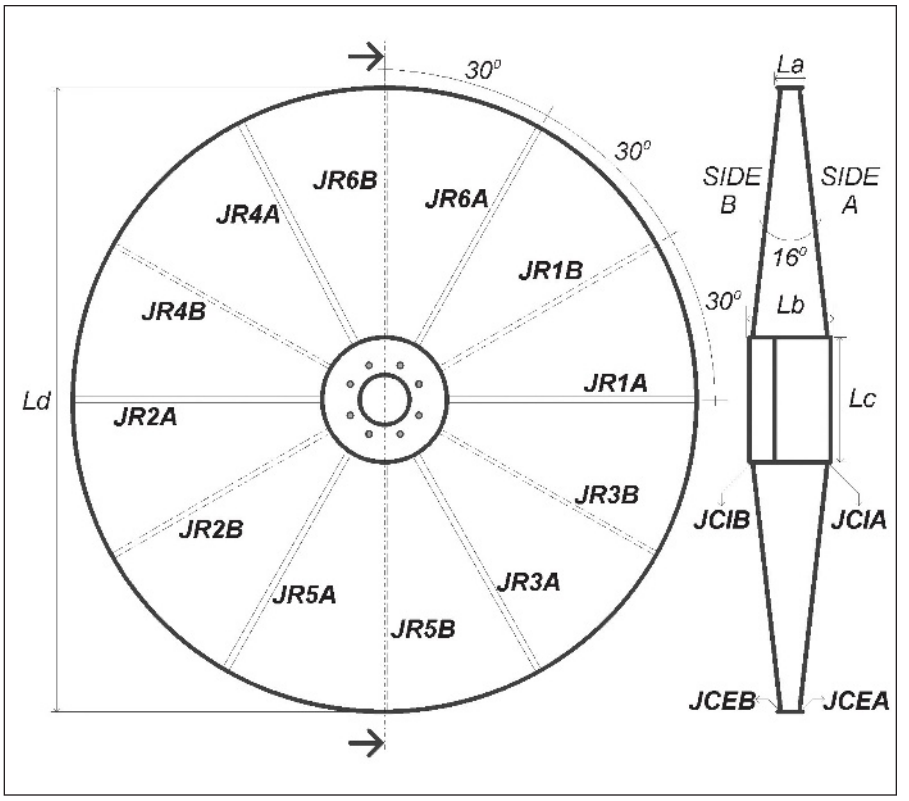

Fig. 3 — Wheel design showing the key dimensions and joints.

Strategies for Automatic Welding

Gas metal arc welding, which was conceived in the 1920s and introduced to the market with positive polarity (DCEP) in the late 1940s, is an example of a welding process that has been continually improved through release of new variations, such as AC GMAW (Ref. 3), CMT GMAW (Ref. 4), SP GMAW (Ref. 5), etc. The main reasons why it has been selected to weld metal tractor wheels are increased productivity and versatility in manufacturing with ferrous alloys, possibilities for process mechanization and automation, and low cost.

Developments and innovations made in the field of welding seek not only to improve processes, but also to remove the welder from the welding environment for health reasons. With an automated welding cell, the welder can perform other tasks such as replacing consumables, operating and supervising operation of other equipment in the automated welding cell, thereby reducing manufacturing time.

Beside the choice of processes, it is necessary to establish a correct execution sequence for welding joints in order to minimize mechanical deformations on the wheel. In this case, the welding direction is from the center outward, in an attempt to more homogeneously distribute the heat of the electric arc on the wheel (Ref. 6).

Thus, the sequence established for single-pass welding of each side of the wheel was performed in accordance with the position of each joint in Fig. 3. Initially, inside circumferential joints are 360-deg continuously welded JCI. Following are welded radial joints toward JCI JCE in the order of JR1 through JR6. Finally, the outer circumference of the joint, JCE, is welded in six portions and always clockwise.

There are two different types of weld joints, radial and circumferential, thus requiring two different welding strategies.

Fig. 4 — Detail of the clearance JR and JCI of a wheel.

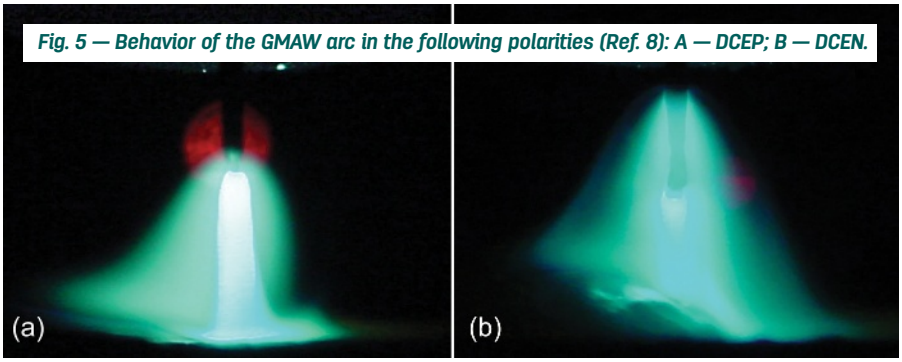

Fig. 5 — Behavior of the GMAW arc in the following polarities (Ref. 8): A — DCEP; B — DCEN.

Radial Joints

The radial joints, JR, are formed from two 2.0-mm-thick plates, welded in the flat position, and with a "V" opening of approximately 10.0 mm — Fig. 4. With these features, the GMAW process with direct current electrode negative (DCEN) polarity, appropriate shielding gas, and a short arc length is the most suitable for having a higher wire melting rate for a given current compared to DCEP polarity.

This fusion rate differential can be explained by the behavior of the electric arc. With DCEN, the arc not only anchors the electrode tip as in DCEP (Fig. 5A), but embraces the electrode widely (Fig. 5B), seeking points where electron emission is favored by the presence of oxides. This feature makes a larger portion of the arc energy transfer to the electrode, increasing its melting in relation to the workpiece.

Thus, the joints can be filled without occurrence of undercuts and with a high-intensity electrical current and with a higher welding speed than in DCEP. Due to the large difference in root opening, it was necessary to oscillate the torch transversely to execute the weld in order to achieve complete joint penetration in a single pass.

Circumferential Joints

Circumferential joints, JCI and JCE, are of the angle type in horizontal welding position and have a 2.0-mm root opening — Fig. 4. These joints are formed from 2.0-mm-thick sheets and 6.35-mm-thick flat bars. Due to the clearance variation, the oscillating movement of the torch in the longitudinal direction of the weld bead does not prevent melt-through. Also, the use of DCEN polarity in place of DCEP does not provide adequate penetration and weld geometry for this type of joint. To overcome these difficulties, a technique to synchronize the polarity of the GMAW process with the longitudinal oscillation movement of the gun was developed — Fig. 6.

For each cycle period T of this technique, the gun moves only a distance d in the direction of welding. Thus, the average speed of the welding, vs, is determined by the following relationship:

$$vs = d/T \qquad (1)$$

In turn, the period T is the sum of two parts:

$$T = tn + tp \qquad (2)$$

tn is the time duration of the DCEN polarity in step 1, advancement of the gun, and tp is duration of the DCEP polarity for gun return in step 2. In this synchronization technique, the dimensionless quantity called duty cycle, D, determines the percentage of the applied DCEN polarity, via the relation

$$D = tn/T \qquad (3)$$

Thus, the percentage of DCEN polarity applied has values in the range $0 < D < 1$ or in percentages, $0\% < D < 100\%$. In step 1, the arc moves over the joint with DCEN polarity, depositing a layer of weld metal in order to seal the joint through the lower heat transfer to the weld pool. The idea is to insert a layer of protection to prevent perforation and undercut during positive polarity of the next step. The forward speed of the arc, va, is given in the following equation:

$$va = \frac{da}{tn} = \frac{2.d}{D.T} = \frac{2.vs}{D} \qquad (4)$$

In step 2, the electric arc returns over the joint with DCEP polarity and deposits material — about half of the protective layer — with greater intensity of heat in the weld pool. Thus, penetration is completed and wettability increases, providing a good weld geometry. The return speed of the arc, vr, is determined at this stage by the equation

$$vr = \frac{-dr}{tp} = \frac{-d}{T.(1-D)} = \frac{-vs}{1-D} \qquad (5)$$

In step 1 of the next cycle, the arc moves back onto the joint with DCEN polarity to deposit material and finish filling over the layer made with DCEP polarity in the previous step.

Because of the deviations in location of the joints in the circumference, it was necessary to use an automatic joint tracking system. The joint outer circumference, (Fig. 7), has a higher location deviation, ± 4 mm in the vertical direction, than does the joint's inner circumference.

The use of an inductive sensor was the most suitable because it is an angled joint in the horizontal welding position (Ref. 9). In this case, two digital, inductive sensors were installed in the welding gun to detect, without physical contact, the presence of the

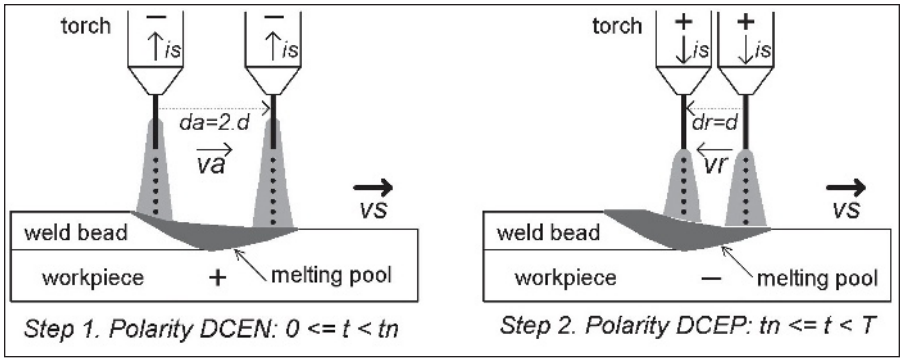

Fig. 6 — Operating steps of the synchronization technique.

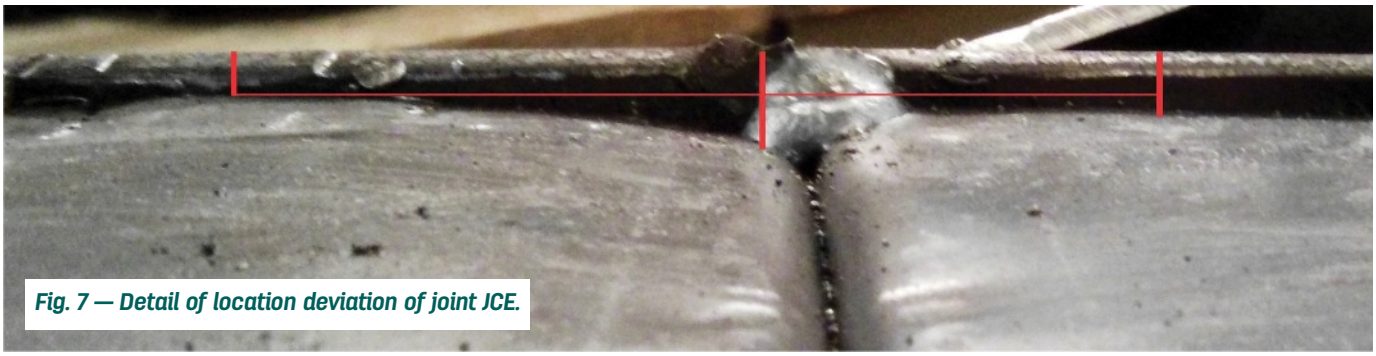

Fig. 7 — Detail of location deviation of joint JCE.

thin steel sheets that make up the joint. Inductive sensors 16 mm in diameter, 5.0-mm nominal detection distance, and 0.4-mm hysteresis were selected. One operates only during welding of the inner circumference of the joint (Fig. 8A), while the other acts only during welding of the outer circumference — Fig. 8B.

To move the gun vertically, a command signal is sent when the inductive sensor detects the thin sheet at a distance smaller than 4.8 mm. If the distance is greater than 5.2 mm, the sensor no longer detects the plate and sends a command to bring the gun vertically back to the joint.

The Welding Cell

To make the operation of automatic welding of wheel structural components more productive and result in better joint quality, efforts were concentrated on designing a specific welding cell. The analysis of commercial welding cells was the starting point for setting the needs of automation strategies for the welding of the wheels. One result of this analysis was discovery of a lack of positioning systems with automatic fixing of the wheels. Therefore, a servo-driven rotary table (Fig. 9) with a clamping device based on a fast lock nut and clamp was developed. This fastening technology facilitates both loading operations. A gear-type worm spindle and 90:1 gear with clearance less than one arc min was used to fit the characteristics of speed and torque of the AC servo motor to driving of the wheels.

The postitioning turntable's main advantage is it allows use of robots that need a smaller work space and a reduced number of degrees of freedom. To minimize costs, it was decided to use a Cartesian robot computer numeric control (CNC) dedicated to welding with four degrees of freedom (Fig. 10) integrated to the rotary positioning table with one degree of freedom. The ability to produce oscillation in the welding gun is this robot's main feature. Gun oscillation can be produced by the movement of only one of its axes or through synchronized movements of two, three, or even all of its axes. This feature allows performance of gun oscillation in the transverse direction, longitudinal direction, or both directions simultaneously (Ref. 10).

All robot axes are moved by DC servo motors with brushes, which in turn, are driven by servo drivers with digital command-type step/direction. The method of motion control for

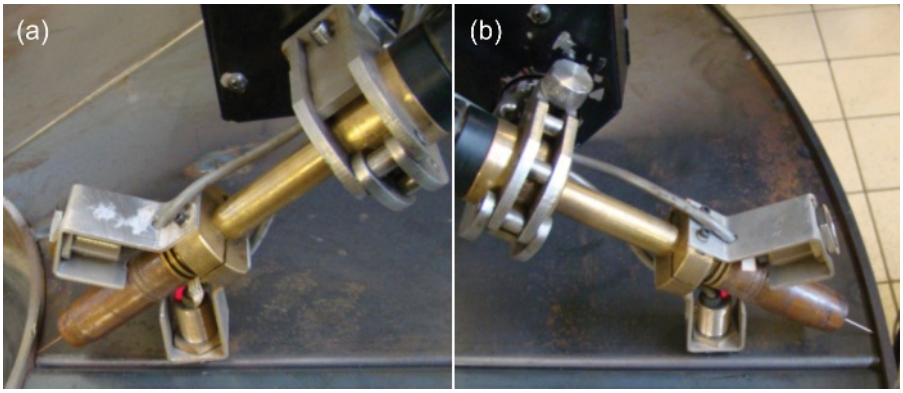

Fig. 8 — Inductive sensors of the tracking system: A — In joint JCI; B — in joint JCE.

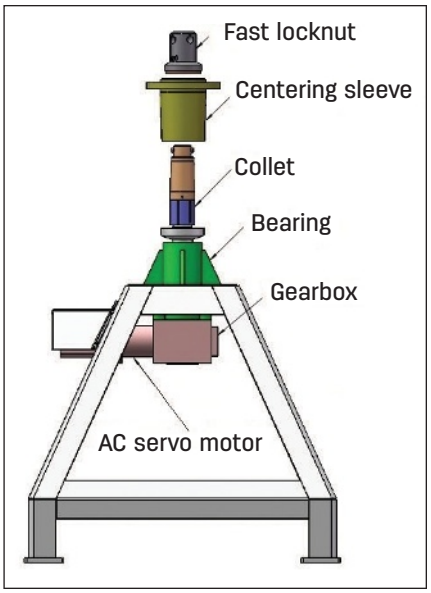

Fig. 9 — Turntable positioning fixture.

both the welding gun and the wheel, as shown in Fig. 11, is similar to that used in CNC machining, facilitating interaction with CAD software. Thus, it is possible to plan complex welding trajectories without programming difficulties. The Mach 3 CNC controller, besides its low cost, has an extremely flexible graphical interface where you can create an environment dedicated to each welding task. This controller also has libraries for touch screens and configuration of a teach pendant more intuitive than the computer keyboard.

To facilitate sequence loading, welding of side A, side shift, welding of side B, wheel unloading, it was decided to install pulleys at the base of the positioning rotary table to move on rails between their two extreme positions. According to the geometrical characteristics of the tractor wheels and the location of its joints, the X-axis of the Cartesian CNC robot was also installed on straight rails, as shown in Fig. 12.

Each axis of this cell has a specific

function in the wheel welding procedure. The X-axis linear displacement performs both a fast upward movement to the initial position of each weld bead and radial welding downward displacement. The operator moves this axis via the correction interface only when there is need for any adjustments in the position of the torch during the welding of circumferential joints. The speed range of this axis is 5 m/min, and its course is 1.2 m.

The linear axis Y is responsible for transverse oscillation movement of the gun during welding of the radius joints and longitudinal oscillation during execution of the circumference welds. This axis has a speed range of 6 m/min with a 120-mm stroke.

The linear axis Z acts during welding of the circumferential joints to correct gun height according to the feedback signal of the inductive sensor. The operator moves this axis via the interface correction only when there is need for any adjustments in the gun position during welding of the radius joints.

The angular axis B is responsible for orientation of the welding gun. This axis has a specific position in relation to normal of the robot's track for welding each joint. For radius joints the value is 10 deg, –55 deg for the joints of the inner circumference, and 50 deg for the joints of the outer circumference. Constructively, this axis has a 360-deg angular displacement around the linear Y axis and a speed range of 300 deg/s.

Operation of the C angular axis differs depending on the type of joint to be welded. During the welding of each radius joint, JR, this axis stops, while the robot moves the gun with transverse oscillation. However, in the girth welding joints, JCE and JCI, this angular axis controls the operating velocity of the wheel, kept constant and equal to the desired welding speed, *vs*, while the robot performs only the longitudinal oscillation of the torch.

Weld Evaluation Criteria

Evaluation criteria applied by the wheel manufacturer considered continuity of the fillet weld, incomplete penetration, and holes in the sheet metal, as well as the geometry of the cross section of each type of welded joint — Fig. 13.

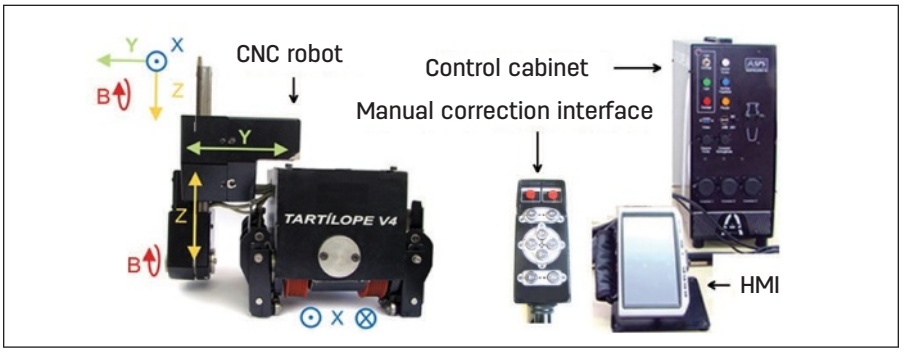

Fig. 10 — CNC Cartesian robot dedicated to welding (Ref. 11).

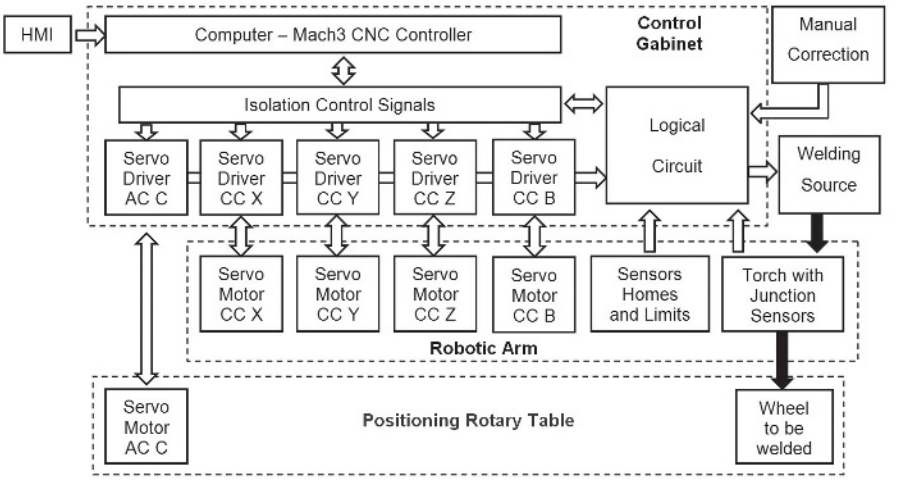

Fig. 11 — Functional block diagram of the welding cell.

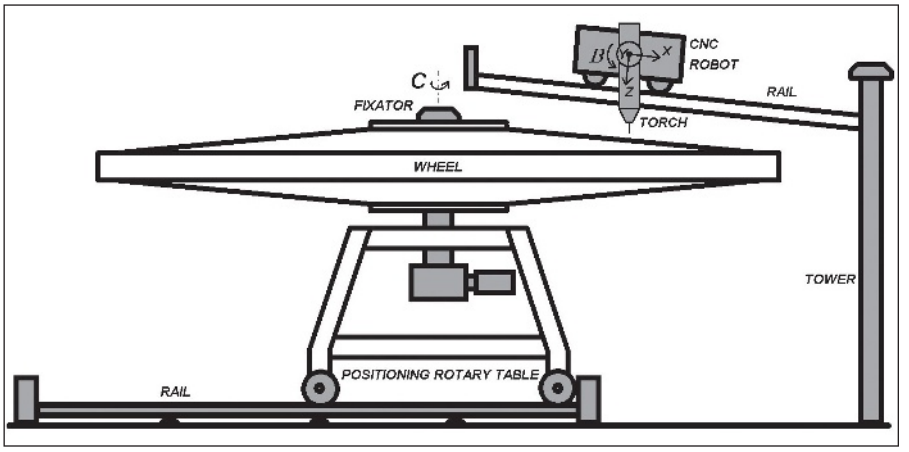

Fig. 12 — Layout of the welding cell.

Analysis of the fillet weld cross section at each joint type is based on the thickness of the thinner sheet that makes up the joint. In the case of a joint formed by joining two plates of thicknesses e1 and e2, the smaller thickness value is called "e." Thus, the minimum and maximum measurements of the weld bead cross sections are bound to the thickness value "e," as shown in Table 1. Note that these criteria have been created over time due to the emergence of problems in the wheels from the weld joints and therefore are more stringent than the criteria established in Ref. 12.

The weld bead is not disqualified by the presence of spatter; however, the occurrence of spatter in large quantities can represent process instability.

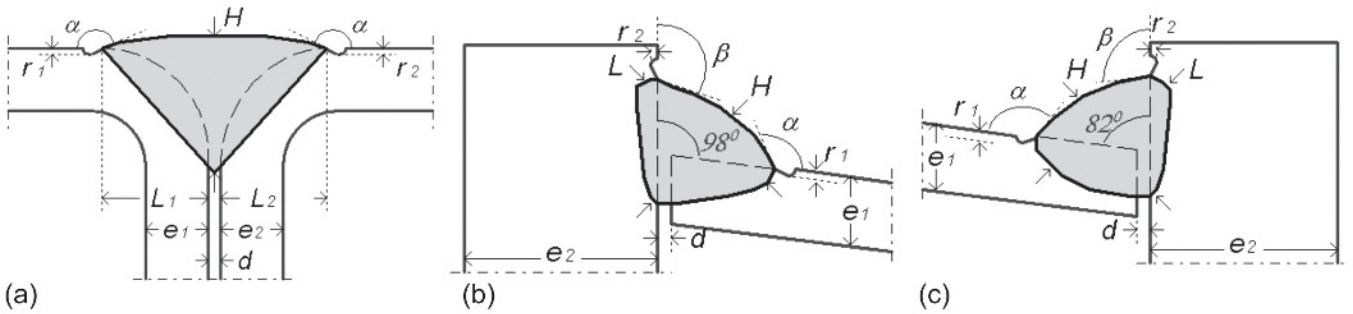

Fig. 13 — Dimensional specifications of joints: A — JR; B — JCI; C — JCE.

In this case, the item was rejected because it could not be guaranteed that the values of the geometric parameters of the cross sections were within the tolerance range.

Experimental Results

After construction of the automated GMAW cell (Fig. 14), the parameter set was obtained (Table 2) for the welding of wheel radius and circumferential joints. These parameters were defined for solid wire 1.2-mm-diameter AWS ER70S-6 with a contact tip-to-work distance of 27 mm. The weld pool was protected by 98% Ar+2% O_2 shielding gas with a flow rate of 18 L/min.

Triangular-type gun oscillation was used for welding of all wheel joints. In the welding of the circumferential joints was applied a duty cycle, D, of 50%; that is, DCEN polarity time length equal to the time length of the DCEP polarity. According to Equations 4 and 5, the forward and return speed of the arc in the joint are, respectively, $va = 4.vs$ and $vr = -2.vs$. In this case, where both the joint and the torch move, the speed of the electric arc in the joint is the joint function of speed,

$$\begin{cases} va = vo + vj = 4.vs \\ vr = -vo + vj = -2.vs \end{cases} \quad (6)$$

Solving the system of Equation 6, one obtains: $vs = vj$ and $vo = 3.vs$. These speeds were used to weld together the circumferential joints of the wheels, as shown in Fig. 15A. The total time required was about 20 min to weld all the joints on one side. This equaled 16.5 min of welding time, 1.5 min of torch positioning time at the beginning of the joints, and 2 min for placement and positioning of the wheel on the table.

After welding, the wheel was subjected to a leak test. The test revealed no leaks in the welded joints on either side of the wheel.

Next, it was verified whether the joints produced met the wheel manufacturer's evaluation criteria. As there was no visible presence of welding defects (Fig. 15B, D, and F), macrographic cross sections of the radius joints weld beads (Fig. 15C), the inner circumferential joints (Fig. 15E), and the outer circumferential joints (Fig. 15G) were made.

Based on dimensional analysis of the macrographs, the joints produced were approved according to the wheel manufacturer's evaluation criteria.

Table 1 — Criteria for Evaluation of the Cross Section of the Weld Beads

Parameters	Tolerable Ranges
Projection of the penetrations: L_1, L_2 (mm)	$L_1 > 1.5e$; $L_2 > 1.5e$
Width of weld bead: L (mm)	$L > 2e$
Height of the weld bead: H (mm)	$H > 1.5e$
Distance between the plates: d (mm)	$d < 0.8e$
Undercuts: r_1, r_2 (mm)	$r_1 < 0.1e$; $r_2 < 0.1e$
Angle reinforcement: α, β (deg)	$\alpha > 120$ deg; $\beta > 90$ deg

Table 2 — Procedure for Welding Structural Wheel Components

Parameters and Operating Details	JR Values	JCI Values	JCE Values
Polarity applied	DCEN	DCEN/DCEP	DCEN/DCEP
Average current applied (A)	–345	–220/300	–220/300
Average voltage obtained (V)	–38.0	–35.0/32.0	–35.0/32.0
Welding speed (m/min)	1.0	0.6	0.6
Wire speed (m/min)	20.0	14.0	14.0
Torch orientation (deg)	10.0	–55.0	50.0
Amplitude of oscillation (mm)	4.0	7.0	7.0
Torch oscillation frequency (Hz)	5.0	2.5	2.5
Use of tracking sensor of joint	no	yes	yes

These macrographs also serve to evaluate the robustness of the welding process in order to seal clearances existing on radius joints with DCEN polarity (Fig. 15C) and circumferential joints with the DCEN and DCEP synchronized with the oscillating motion of the torch — Fig. 15E. Another important detail is the overlap of 10 mm on the circumference joint weld bead, as shown in Fig. 15F, which is required to ensure tightness of the wheels.

Conclusions

Computer numerical controlled programming technology coupled with the use of the Mach3 controller provided easy, quality integration between the positioning turntable and the dedicated Cartesian welding robot. With this technology, it was possible to run any operator-performed positioning correction of the electric arc during welding. Furthermore, the positioning rotary table was properly controlled in two different modes: position in the radial joints and speed in the circumferential joints.

The GMAW process with DCEN polarity and transverse oscillation of the gun is a good alternative for single-pass welding of thin-sheet radius joints. The respective procedure produces uniform weld beads free of defects, and increases productivity with improved sealing than in classic GMAW with DCEP polarity.

The use of an inductive sensor for monitoring the weld together with the synchronization of GMAW polarity with the direction of movement of the electric arc provided the desired robustness and repeatability to achieve high-quality joints between plates of different thicknesses and with clearance in the circumferential joints of the wheel. However, this technology requires devices that communicate with each other and a good dedication in qualifying the set of variables and parameters of the welding process and of the automatic wheel and gun displacement.

Fig. 14 — The automated GMAW tractor wheel cell.

Weld joints run with the techniques described and according to a planned sequence not only met the evaluation criteria of the manufacturer, but also provided tightness and minimal deformation in the mechanical structure of the wheels.

With the development of an automated welding cell to weld structural wheel components, a 28.2% reduction in welding time and an increase in productivity of approximately 100% was achieved as compared to conventional GMAW with a manual gun. WJ

Acknowledgments

The authors wish to thank Brasélio for the opportunity afforded and the professionals of the Labsolda for technical support.

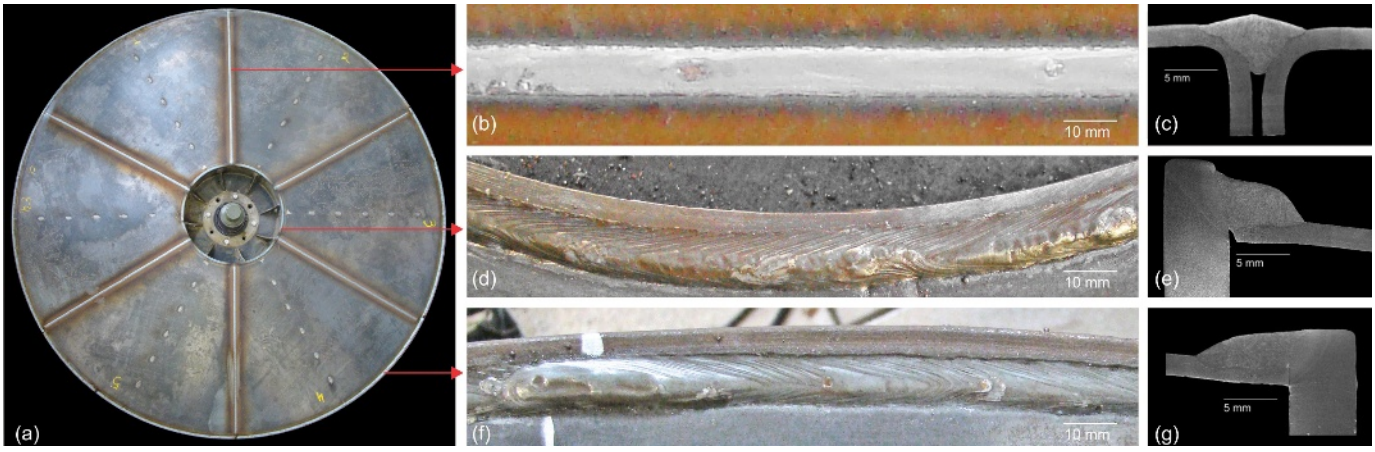

Fig. 15 — A — Weld beads deposited in the joints of side A of the largest wheel; B — weld bead JR; C — macrograph of the cross section JR; D — weld bead JCI; E — macrograph of the cross section JCI; F — weld bead JCE; G — macrograph of the cross section JCE.

References

1. Hemmer, M. H. 2005. Reinforced wheel structured for agricultural machine. *Journal of Industrial Property* 1823, 74. Int Cl[B60B] 15/00. BR. MU 8401928-0.

2. Kaneko, Y., Yamane, S., and Oshima, K. 2009. Numerial simulation of MIG weld pool in switchback welding. *Welding in the World* 53(11/12): 333–341.

3. Ueyama, T., Tong, H., Harada, S., Passmore, R., and Ushio, M. 2005. AC pulsed GMAW improves sheet metal joining. *Welding Journal* 84(2): 40–46.

4. Pickin, C. G., Williams, S. W., and Lunt, M. 2011. Characterization of the cold metal transfer (CMT) process and its application for low dilution cladding. *Journal of Materials Processing Technology* 211(3): 496–502.

5. Dutra, J. C., Puhl, E. B., Bonacorso, N. G., and Silva, R. H. G. 2013. Improving surfacing performance with GMAW. *Welding Journal* 92(5): 42–47.

6. Tsai, C. L., Park, S. C., and Chen, W. T. 1999. Welding distortion of a thin-plate panel structure. *Welding Journal* 78(5): 156-s to 165-s.

7. Souza, D., Rezende, A. A., and Scotti, A. 2009. A qualitative model to explain the polarity influence on the fusion rate in the MIG/MAG process. *Revista Soldagem & Inspeção* 14(3): 192–198.

8. Cirino, L. M. 2009. Study on the effects of polarity in direct and alternate current TIG and MIG/MAG welding processes. Master's thesis. PosMec/ UFSC, Florianópolis, Brazil.

9. Norrish, J. 2006. *Advanced Welding Processes: Technologies and Process Control*. Cambridge, England: Woodhead Publishing. pp. 203–216.

10. Yamane, S., Yamamoto, H., Kaneko, Y., and Oshima, K. 2006. Sensing and seam tracking of welding line in backingless V groove welding. *Science and Technology of Welding and Joining* 11(5): 586–592.

11. Carvalho, R. S. 2009. CNC robot for automation of MIG/MAG welding in positions and situations of extreme difficulty. Master's thesis. PosMec/UFSC, Florianópolis, Brazil.

12. ANSI/AWS D1.1/D1.1M: 2004, *Structural Welding Code — Steel*. Miami, Fla.: American Welding Society. p. 499.